Delft University of Technology

Thermal Modelling and Experimental Validation for Research on Medium Voltage DC Cables

Shekhar, A.; Feng, X.; Hebner, R.; Gattozzi, A.; Strank, S.; Mor, A.; Ramirez-Elizondo, L.; Bauer, P.

DOI
10.1109/PESGM.2017.8274559

Publication date
2018

Document Version
Accepted author manuscript

Published in
2017 IEEE Power and Energy Society General Meeting, PESGM 2017

Citation (APA)
Shekhar, A., Feng, X., Hebner, R., Gattozzi, A., Strank, S., Mor, A., Ramirez-Elizondo, L., & Bauer, P. (2018). Thermal Modelling and Experimental Validation for Research on Medium Voltage DC Cables. In *2017 IEEE Power and Energy Society General Meeting, PESGM 2017* (Vol. 2018-January, pp. 1-5). IEEE. https://doi.org/10.1109/PESGM.2017.8274559

Thermal Modelling and Experimental Validation for Research on Medium Voltage DC Cables

A. Shekhar, X. Feng, R. Hebner, A. Gattozzi, S. Strank, A. Mor, L. Ramírez-Elizondo and P. Bauer
Center for Electromechanics, University of Texas, Austin & Delft University of Technology, Netherlands
a.shekhar@tudelft.nl

***Abstract*—The thermal behavior of medium voltage dc cables can find useful applications for efficient and capacity enhanced operation in cities as well as compact power transmission on all electric ships. Concepts such as dynamic current and voltage rating, difference in thermal proximity in ac and dc operation, pulsed load application and thermal degradation with enhanced dc voltage; all are interlaced with the crucial temperature profile of insulated conductors. This paper develops a theoretical thermal model to highlight the possibility of dynamic current rating with pulsed loads. Further, a novel idea of imposing a thermal profile on cables for dc partial discharge testing is discussed. For this purpose a heat transfer model for a segmented cable is developed and experimentally validated.**

I. Applications of the Insulated Conductor Thermal Study

In all electric ships and future cities with emerging intensive green energy consumers like electric vehicles, application of medium voltage dc (MVdc) cables is finding traction [1], [2].

Due to the compactness and efficient power transmission with dc cable operation as compared to ac, the weight and volume of cabling infrastructure can be minimized, thus enhancing the ability of ships to carry critical payloads [1]. It is recognized that the expected cable usage is a fraction of the ship's operational lifetime, particularly in the case of high powered intermittent pulsed loads. Thereby, from the thermal point of view, it is possible to reduce the chosen conductor size further.

In cities, with rapidly increasing power demand, the critical underground cable infrastructure linking the inner city radial network with the outer substation is getting overloaded [2]. It is highlighted that by refurbishing the existing ac infrastructure under dc conditions, capacity enhancement can be achieved, thus avoiding the digging and installation costs.

At the center of the concepts presented in [1], [2], with applications such as dynamic current and voltage rating, thermal proximity effects and enhanced dc voltage operation, is the thermal behaviour of the cross linked polyethylene (XLPE) insulated conductor, its interaction with the electric field profile and the insulation degradation.

With this larger picture in mind, the focus of this study was to develop a MVdc cross linked polyethylene cable thermal model to enable the design of cable degradation test setups under thermal heating and validate it through experiments.

A. Dynamic Current Rating

The study of intelligent overloading of distribution network by dynamic current rating, making use of thermal inertia of different system components is presented in [3], [4]. In [5], this concept is used to under design the chosen converter for PV applications, making use of the intermittent nature of PV energy generation. Furthermore, in [1] it is pointed that even if the temperature imposed on the cable insulation exceeds certain limits for short duration, the thermal degradation is not significantly different. This can be exploited for cable conductor downsizing in ship power system applications. For pulsed loads, which require cable operation only for a short duration, this concept can be particularly advantageous and is explored in Section II.

B. AC to DC Voltage Enhancement

The maximum efficiency and capacity enhancement with the dc operation of medium voltage ac cables comes from voltage enhancement by a factor of $\sqrt{2}$ [2]. However, the differences of ac and dc operation on the insulation lifetime and partial discharges, particularly under higher temperature, need more attention. The general experimental set-up used to measure the partial discharges is shown in Fig. 1.

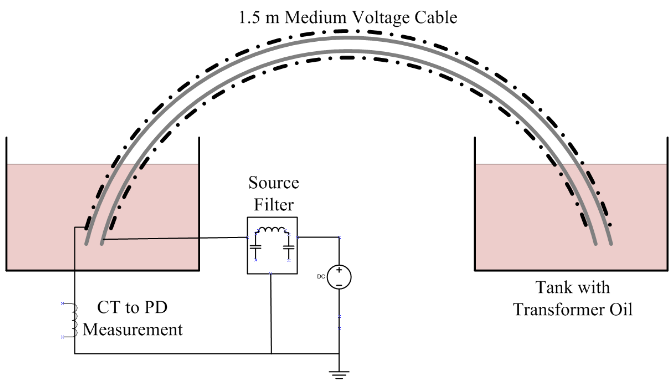

Fig. 1. Experimental setup for partial discharge measurements.

In practice, imposing a controlled temperature along the cable length is not a straightforward task. This issue is explored in Section III.

II. Dynamic Current Rating for Pulsed Loads

A. Resistive Heating Thermal Model

In the cable test (electrical and thermal), the temperature gradient in the cable insulation and conductor temperature are two important factors. Resistive heating, injecting high current on the inner conductor, is an effective way to emulate the cable thermal environment. While this emulates service conditions, it is not always the most practical approach for laboratory testing. In the high voltage test in this investigation, for example, the inner conductor is grounded and high voltage electrode is connected to the metal sheath for safety reason. The cross section of a typical medium voltage single-conductor cable is shown in Fig. 2.

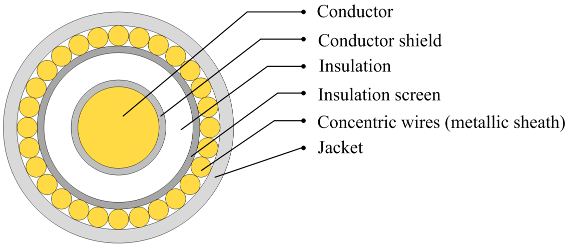

Fig. 2. Illustration for cross-section of a cable.

In order to derive an analytical method to study the cable thermal behavior, the thermal network analogy is applied due to the similarity between heat flow and electric current flow. As the electric current flow is induced by the electric potential difference, the heat flow is induced by temperature difference. The thermal resistance is defined as the materials ability to impede heat flow; the thermal capacitance is defined as the materials ability to store heat. Thus, a thermal circuit can be modeled by an analogous electric circuit [6]. The thermal network analogs for cables have been adopted by many international standards [7]- [10].

The thermal network for the cable with electrical analogy is shown in Fig. 3. The heat generated by the electric current flow I in the conductor is modelled as I^2R losses where R is the DC resistance per meter on the cable. Q_{C} is the thermal capacitance of conductor. Q_{CS} is the thermal capacitance of the conductor shield. Q_{i1}, Q_{i2}, Q_{i3}, and Q_{i4} are the equivalent thermal capacitance of the cable insulation layer. T_1 is the thermal resistance of the cable insulation layer. Q_{IS} is the thermal capacitance of the insulation screen. Q_{S} is the thermal capacitance of the metallic sheath. Q_{J1} and Q_{J2} are the equivalent thermal capacitance of the cable jacket. T_3 is the thermal resistance of the cable jacket. T_4 is the thermal resistance of the cable external environment. θ_{amb} is the ambient temperature of the cable. The calculation procedure for these circuit coefficients are given in [7] and [8]. In DC cables, the dielectric losses and sheath losses are equal to 0. This thermal network model can be used to estimate the cable conductor temperature using electrical current flow and ambient temperature as inputs.

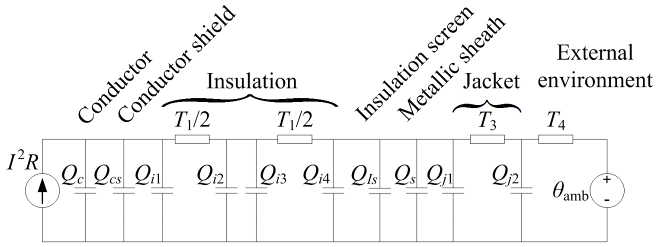

Fig. 3. Thermal network for the cable with electrical analogy.

The thermal resistivity of semiconductor and metal is very small. The thickness of the conductor shield and insulation screen is very also small. Thus, the thermal resistances of conductor shield, insulation screen and metallic sheath are not included in the cable thermal network. The thermal capacity of semiconductor and metal is not small, so the thermal capacitance of conductor shield, insulation screen and metallic sheath are included in the cable thermal network. To simplify the analysis, the coefficients in cable thermal network model can be lumped and the new thermal network model is shown in Fig. 4. θ_{a}, θ_{b}, θ_{c}, and θ_{d} are the conductor temperature, insulation temperature, metallic sheath temperature, and jacket temperature, respectively.

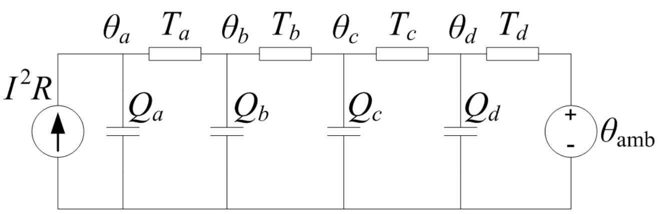

Fig. 4. Thermal network for the cable with lumped parameters.

The state space representation of the thermal equivalent circuit is given in (1),

$$\begin{bmatrix} \dot{\theta}_{\mathrm{a}} \\ \dot{\theta}_{\mathrm{b}} \\ \dot{\theta}_{\mathrm{c}} \\ \dot{\theta}_{\mathrm{d}} \end{bmatrix} = A \begin{bmatrix} \theta_{\mathrm{a}} \\ \theta_{\mathrm{b}} \\ \theta_{\mathrm{c}} \\ \theta_{\mathrm{d}} \end{bmatrix} + \begin{bmatrix} \frac{R}{Q_{\mathrm{a}}} & 0 \\ 0 & 0 \\ 0 & 0 \\ 0 & \frac{1}{T_{\mathrm{d}}Q_{\mathrm{d}}} \end{bmatrix} \begin{bmatrix} I^2 \\ \theta_{\mathrm{amb}} \end{bmatrix} \tag{1}$$

Where,

$$A = \begin{bmatrix} \frac{-1}{T_{\mathrm{a}}Q_{\mathrm{a}}} & \frac{-1}{T_{\mathrm{a}}Q_{\mathrm{a}}} & 0 & 0 \\ \frac{1}{T_{\mathrm{a}}Q_{\mathrm{b}}} & \frac{-1}{T_{\mathrm{a}}Q_{\mathrm{b}}} - \frac{1}{T_{\mathrm{b}}Q_{\mathrm{b}}} & \frac{1}{T_{\mathrm{b}}Q_{\mathrm{b}}} & 0 \\ 0 & \frac{1}{T_{\mathrm{b}}Q_{\mathrm{c}}} & \frac{-1}{T_{\mathrm{b}}Q_{\mathrm{c}}} - \frac{1}{T_{\mathrm{c}}Q_{\mathrm{c}}} & \frac{1}{T_{\mathrm{c}}Q_{\mathrm{c}}} \\ 0 & 0 & \frac{1}{T_{\mathrm{c}}Q_{\mathrm{d}}} & \frac{-1}{T_{\mathrm{c}}Q_{\mathrm{d}}} - \frac{1}{T_{\mathrm{d}}Q_{\mathrm{d}}} \end{bmatrix}$$

The inputs for this model include electric current flow on the cable and the cable ambient temperature. Other coefficients can be calculated based on cable dimension and thermal resistivity/capacity parameters.

To better understand the cable thermal behavior, we compare the temperature changes of a dc cable under two different loading scenarios. A 3/0 TRXLPE 15 kV 100 % insulation cable with 5 mm insulation thickness is used in the study. The cable is installed in open air with ambient air temperature of 20 °C. The ampacity of the cable (from manufacture datasheet) is 270 A in duct. It is assumed that the ambient air temperature is always equal to 20 °C.

In the first scenario, a sustained current flow with 300 A is applied to the DC cable for 2 hours. The simulated temperature dynamics as per (1) are shown in Fig. 5.

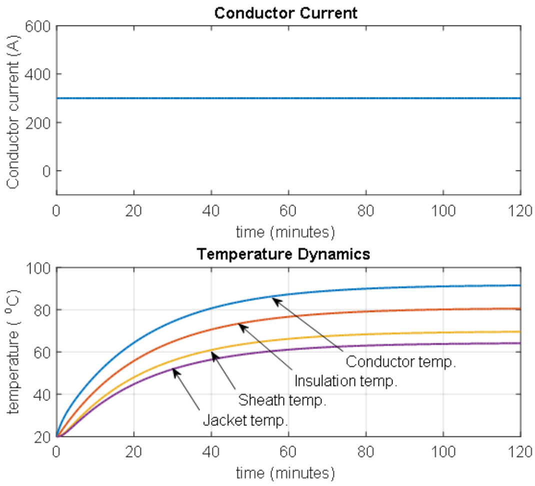

Fig. 5. The thermal behavior of a cable with sustained current flow.

The cable conductor temperature gradually converges to the steady state at 90 °C in around one hour. The slow thermal behavior is caused by the cable thermal capacitance. After a current change happens, the cable temperature takes a certain time to converge to the steady state. The time constant is usually determined by the cable size.

In the second scenario, a pulsed current flow as shown in Fig. 6 is applied to the DC cable. The pulse current has 365 A from 0-20 min and then drops to 0. The temperature dynamics are described in Fig. 6.

When the current is applied, the cable temperature increases from 20 °C. In this case, the maximum cable conductor temperature is also 90 °C, but more that 20 % higher current was imposed.

The cable ampacity is defined as the maximum allowed sustained current on a cable without causing cable overheating with the worst case ambient conditions. If the cable conductor temperature is less than the rated maximum conductor temperature, the cable loading can exceed the rated current for certain amount of time until the conductor temperature reaches the rated maximum conductor temperature. This concept is also known as "Dynamic Current Rating".

Pulsed loads on ship power systems draw current intermittently. The duty ratio of the pulse is usually small. This feature provides a good opportunity to reduce the cable size for pulsed loads.

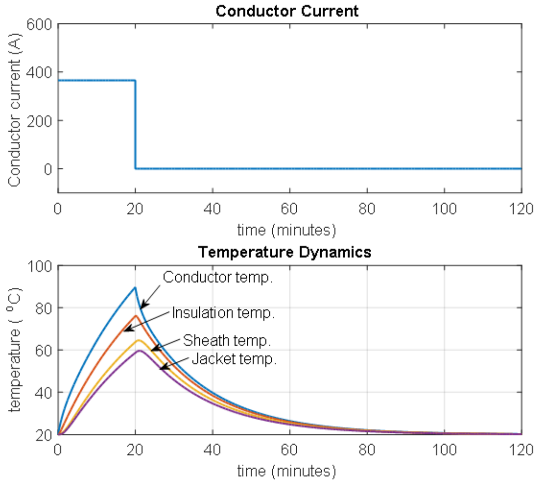

Fig. 6. The thermal behavior of a cable with pulsed current flow.

III. Imposing Thermal Profile for Temperature Dependent Partial Discharge Measurement

One would like to study field conditions under high temperature for cable degradation test setup shown in Fig 1. With short samples, this is challenging. It requires a high power supply to provide both heating and the appropriate electric field distribution in the cable. Alternatively this could be done synthetically with one supply providing the heating and the other providing the electric field.

In this resistive heating method, the connectors submerged in the oil in the set-up shown in Fig. 1 have a finite contact resistance which can cause excessive heating during high current operation. Apart from safety concerns, extended high current operation for thermal degradation tests is difficult, particularly at laboratory scale. Further, the high voltage that needs to be imposed has to be in the opposite direction as in actual cable operation, such that the inner conductor is grounded and the outer metal shield is at raised voltage. This is different than normal high voltage operation of cables and may lead to different partial discharge behavior to be accounted for.

Another alternative is that the thermal control could be supplied in other ways and only the electric field is supplied electrically. This approach is explored in this paper.

A. *Proposed idea using submerged end point heating*

The idea proposed in this paper is that of imposing a particular temperature on the cable by heating the oil in which both the end points are submerged as depicted in Fig. 7.

The center conductor and the shield conductors provide longitudinal averaging while the insulation material is such a poor conductor that radial cooling is dominated by conduction along the length and thus, the temperature at the mid point of

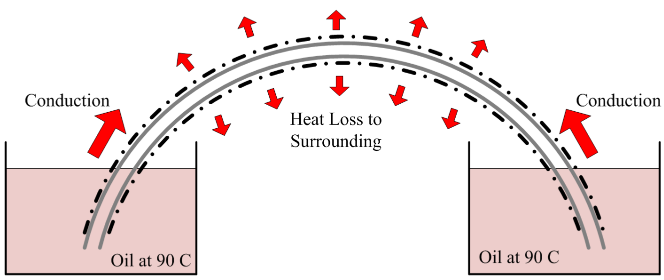

Fig. 7. Thermal flow illustration of proposed heating scheme.

the cable sample rises. Nevertheless, the rise time and steady state value of this point depends on cable parameters and ambient conditions, which must be carefully studied to obtain a reasonable estimate.

B. Segmented cable thermal model and experiments

The equivalent thermal circuit of the system is shown in Fig. 8.

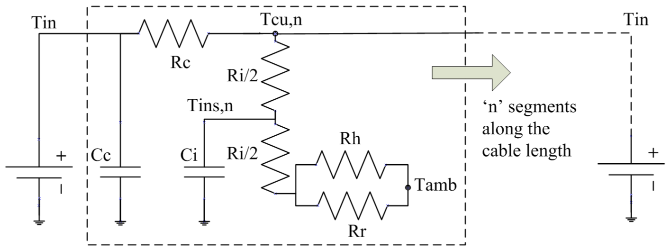

Fig. 8. Equivalent circuit for segmented heat flow in cable with both ends immersed in hot fluid.

The cable is considered to be made of 'n' segments along its length and is heated from both ends at temperature T_{in}. R_{c} and C_{c} and the thermal resistance and capacitance of a copper segment, while R_{i} and C_{i} are lumped thermal resistance and capacitance of each insulation segment. Radial cooling by convection is R_{h} and radiation is R_{r} to air at ambient temperature T_{amb}.

The state space representation for heat flow in segmented cable with radial cooling is given in (2),

$$\begin{bmatrix} \dot{T}_{\text{cu},1} \\ \cdot \\ \cdot \\ \dot{T}_{\text{cu,n}} \\ \dot{T}_{\text{ins},1} \\ \cdot \\ \cdot \\ \dot{T}_{\text{ins,n}} \end{bmatrix} = \begin{bmatrix} A_{\text{k1}} & A_{\text{k2}} \\ A_{\text{k3}} & A_{\text{k4}} \end{bmatrix} \begin{bmatrix} T_{\text{cu},1} \\ \cdot \\ \cdot \\ T_{\text{cu,n}} \\ T_{\text{ins},1} \\ \cdot \\ \cdot \\ T_{\text{ins,n}} \end{bmatrix} + \begin{bmatrix} \frac{1}{R_{\text{c}}C_{\text{c}}} & 0 \\ 0 & \cdot \\ \cdot & \cdot \\ \frac{1}{R_{\text{c}}C_{\text{c}}} & 0 \\ 0 & \frac{1}{(\frac{R_{\text{i}}}{2}+R_{\text{h}})C_{\text{i}}} \\ \cdot & \cdot \\ \cdot & \cdot \\ 0 & \frac{1}{(\frac{R_{\text{i}}}{2}+R_{\text{h}})C_{\text{i}}} \end{bmatrix} \begin{bmatrix} T_{\text{in}} \\ T_{\text{amb}} \end{bmatrix} \tag{2}$$

Where, A_{k1}, A_{k2}, A_{k3}, A_{k4} are nxn matrices given by,

$$A_{\text{k1}} = \begin{bmatrix} \frac{-2}{R_{\text{c}}C_{\text{c}}} + \frac{-2}{R_{\text{i}}C_{\text{c}}} & \frac{1}{R_{\text{c}}C_{\text{c}}} & 0 & \cdot & \cdot \\ \frac{1}{R_{\text{c}}C_{\text{c}}} & \frac{-2}{R_{\text{c}}C_{\text{c}}} + \frac{-2}{R_{\text{i}}C_{\text{c}}} & \frac{1}{R_{\text{c}}C_{\text{c}}} & 0 & \cdot \\ 0 & \frac{1}{R_{\text{c}}C_{\text{c}}} & \cdot & \cdot & \cdot \\ \cdot & 0 & \cdot & \cdot & \cdot \\ \cdot & \cdot & \cdot & \cdot & \frac{1}{R_{\text{c}}C_{\text{c}}} \\ 0 & 0 & 0 & \frac{1}{R_{\text{c}}C_{\text{c}}} & \frac{-2}{R_{\text{c}}C_{\text{c}}} + \frac{-2}{R_{\text{i}}C_{\text{c}}} \end{bmatrix}$$

$$A_{\text{k2}} = diag\left(\frac{2}{R_{\text{i}}C_{\text{c}}}\right)_{\text{nxn}}$$

$$A_{\text{k3}} = diag\left(\frac{2}{R_{\text{i}}C_{\text{i}}}\right)_{\text{nxn}}$$

$$A_{\text{k4}} = -diag\left(\frac{1}{(\frac{R_{\text{i}}}{2}+R_{\text{h}})C_{\text{i}}} + \frac{2}{R_{\text{i}}C_{\text{i}}}\right)_{\text{nxn}}$$

A total of 200 state space equations are simulated for a 1.5 m cable with 100 segments to estimate the temperature rise time and steady state temperature of the mid point as shown in Fig. 9. The theoretical maximum temperature rise at the midpoint is calculated to be about 46 °C in steady state reached in 1 to 1.5 hr. The delay in rise of mid point temperature (solid blue) is due to segmented heat transfer.

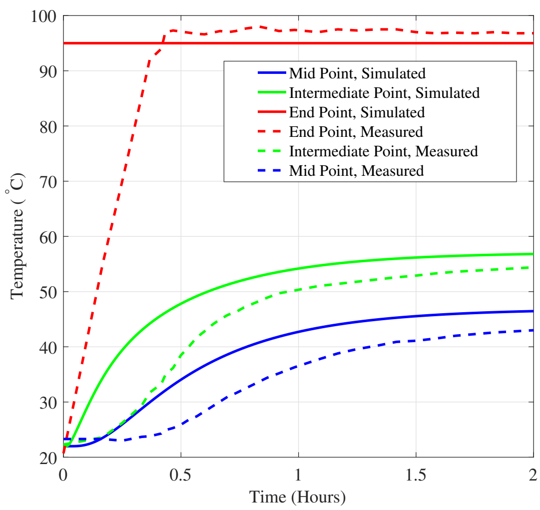

Fig. 9. Comparison of simulated and measured temperature rise of a 85 mm^2, 1.5 m XLPE cable with end points heated at 95 °C.

While the actual high voltage experiments would use oil heating, the model is validated using set up in similar conditions with end points immersed in heated water. It can be observed that it takes some time to heat up the ends, which causes more delay in reaching steady state. The temperature is measured using thermocouples drilled right to the inner conductor at the midpoint and the intermediate point (half way between the end and mid point). Fig. 9. shows the temperature evolution and steady state value, which correlate well with the theoretical results.

In order to get a higher steady state value, several options are available:

- Increasing the ambient temperature to mimic actual con-

ditions can reduce cooling.
- Increasing the conductor area can enhance the longitudinal heat conductivity relative to the redial cooling.
- Decreasing the length of cable sample.
- Thermally insulating the outer surface of the cable.

The thermal test was conducted again after thermally insulating the cable and is shown in Fig. 10. It can be observed that the steady state value at midpoint is about 63 °C which is 20 °C higher than previous case.

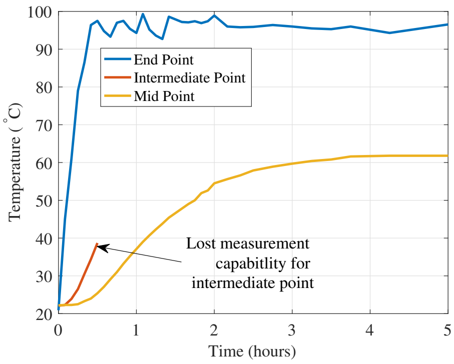

Fig. 10. Experimental Results for a 85 mm^2, 1.5 m XLPE cable thermally insulated along its length.

However, thermally insulating the cable reduces the temperature gradient along the electrical insulation. Space charge accumulation depends on the temperature distribution. This means both the electric field and the thermal gradients must be known well for cable degradation study.

One way to increase the mid point temperature without thermal insulation is by minimising the cable sample length, as shown in Fig. 11. But the concern here is too maintain enough clearance for high voltage experiments.

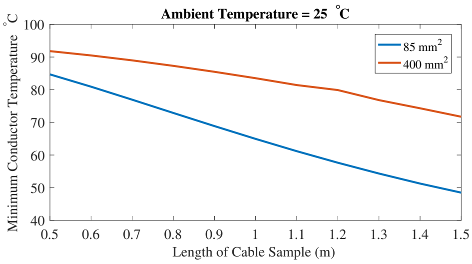

Fig. 11. Minimum conductor temperature rise at mid point with sample length.

Other methods would be to increase conductor cross section to aid lateral conduction, and increasing the ambient air temperature to reduce radial cooling. Simulation results showing the temperature along the cable length for different cable area and ambient temperatures is shown in Fig. 12.

Increase in area is a good way of improving the highest temperature at the mid point and minimizing the lateral temperature gradient along the conductor length. However, for the same insulation thickness, the no load electric field profile is lower for greater copper area.

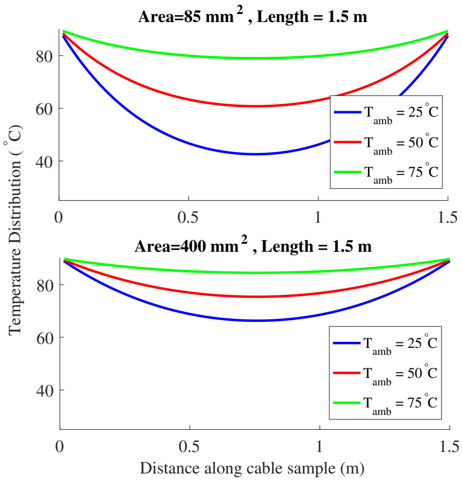

Fig. 12. Conductor area and ambient temperature dependence of thermal gradient along cable length.

IV. CONCLUSIONS

The purpose of the thermal model described in this study enables us to conduct cable degradation tests under higher temperature, while avoiding high current operation resistive heating using dual power supplies. Thermal test results support the accuracy of the predictive MVdc cable thermal model. The combination of modeling and experiments make this an attractive approach to pursue. Possibility of improving the thermal profile using thermal insulation or varying the sample length, conductor area and ambient temperature is explored.

REFERENCES

[1] R. E. Hebner, A. L. Gattozzi and S. D. Pekarek, “Performance assurance for DC cables for electric ships,” *Electric Ship Technologies Symposium (ESTS), IEEE,* Alexandria, VA, 2015, pp. 343-348.

[2] A. Shekhar, E. Kontos, A. Rodrigo Mor, L. Ramírez-Elizondo and P. Bauer, “Refurbishing Existing MVAC Distribution Cables to Operate Under DC Conditions,” *Power Electronics and Motion Control Conference and Exposition,* 17th International, Varna, 2016.

[3] X. Feng and M. J. Mousavi, “Study of intelligent overloading in power delivery systems, ” *IEEE PES General Meeting — Conference Exposition,* National Harbor, MD, 2014, pp. 1-5.

[4] X. Feng and M. J. Mousavi, “A framework for intelligent feeder overloading,” *IEEE PES TD Conference and Exposition,* Chicago, IL, USA, 2014, pp. 1-5.

[5] G.R. Chandra Mouli, P. Bauer, M. Zeman, “System design for a solar powered electric vehicle charging station for workplaces,” *Applied Energy,* Volume 168, 15 April 2016, Pages 434-443.

[6] George J. Anders, “Rating of Electric Cables in Unfavorable Thermal Environment,” *Wiley-IEEE Press,* 2005.

[7] Electrical Cable Calculation of the Current Rating, IEC 60287-1-1, “Current rating equation (100% load factor) and calculation of losses general” second edition, 2006.

[8] Electrical Cable Calculation of the Current Rating, IEC 60287-2-1, “Thermal resistance calculation of thermal resistance” , 2006.

[9] Current Ratings of Cables for Cyclic and Emergency Loads, Working Group 02 of Study Committee 21 (HV Cables), 1972.

[10] Calculation of the Cyclic and Emergency Current Rating of Cables Part 1: Cyclic Rating Factor for Cables up to and including 18/30 (36) kV.